TECHNICAL SPOTLIGHT
Selective and regulated gene expression in murine Purkinje cells by *in utero* electroporation

Jun Nishiyama,[1,*,†] Yukari Hayashi,[1,2,†] Toshihiro Nomura,[1,2,3] Eriko Miura,[1,2] Wataru Kakegawa[1,2] and Michisuke Yuzaki[1,2]

[1]Department of Physiology, School of Medicine, Keio University, 35 Shinanomachi, Shinjuku-ku, Tokyo 160-8582, Japan
[2]Core Research for Evolutional Science and Technology (CREST), Japan Science and Technology Corporation, Saitama, Japan
[3]Department of Pediatrics, School of Medicine, Keio University, 35 Shinanomachi, Shinjuku-ku, Tokyo 160-8582, Japan

Abstract

Cerebellar Purkinje cells, which convey the only output from the cerebellar cortex, play an essential role in cerebellar functions, such as motor coordination and motor learning. To understand how Purkinje cells develop and function in the mature cerebellum, an efficient method for molecularly perturbing them is needed. Here we demonstrate that Purkinje cell progenitors at embryonic day (E)11.5 could be efficiently and preferentially transfected by spatially directed *in utero* electroporation (IUE) with an optimized arrangement of electrodes. Electrophysiological analyses indicated that the electroporated Purkinje cells maintained normal membrane properties, synaptic responses and synaptic plasticity at postnatal days 25–28. By combining the L7 promoter and inducible Cre∕loxP system with IUE, transgenes were expressed even more specifically in Purkinje cells and in a temporally controlled manner. We also show that three different fluorescent proteins could be simultaneously expressed, and that Bassoon, a large synaptic protein, could be expressed in the electroporated Purkinje cells. Moreover, phenotypes of *staggerer* mutant mice, which have a deletion in the gene encoding retinoid-related orphan receptor α (RORα1), were recapitulated by electroporating a dominant-negative form of RORα1 into Purkinje cells at E11.5. Together, these results indicate that this new IUE protocol, which allows the selective, effective and temporally regulated expression of multiple foreign genes transfected into Purkinje cell progenitors *in vivo*, without changing the cells' physiological characteristics, is a powerful tool for elucidating the molecular mechanisms underlying early Purkinje cell developmental events, such as dendritogenesis and migration, and synaptic plasticity in mature Purkinje cells.

Introduction

The cerebellum has served as an important system for studying neurodevelopment and information processing because of its well-characterized circuits, which consist of relatively few cell types (Altman & Bayer, 1997). Cerebellar Purkinje cells have been prominently featured in these studies. For example, the long-term depression (LTD) of synaptic transmission at parallel fiber (PF)–Purkinje cell synapses is thought to underlie certain forms of motor learning in the cerebellum (Ito, 1989). Furthermore, the unique shape of Purkinje cell dendrites makes them especially useful for investigating the molecular mechanisms underlying neuronal dendrite development (Sotelo & Dusart, 2009). Therefore, various methods have been developed to molecularly perturb Purkinje cells by expressing exogenous genes.

Although Purkinje cells can be transgenically targeted by using the L7 (Pcp2) promoter (Oberdick *et al.*, 1990; Smeyne *et al.*, 1991; Tomomura *et al.*, 2001), the selection of mouse lines expressing high levels of transgenes can be time-consuming and labor-intensive (Yuzaki, 2005). Furthermore, the L7 promoter turns on relatively late in postnatal development (Smeyne *et al.*, 1991; Tomomura *et al.*, 2001), making it difficult for researchers to perturb early developmental events. As an alternative approach, viral vectors, including adenovirus (Hashimoto *et al.*, 1996), adeno-associated virus (AAV) (Kaemmerer *et al.*, 2000), herpes simplex virus (Agudo *et al.*, 2002), Sindbis virus (Kohda *et al.*, 2007) and lentivirus (Torashima *et al.*, 2006), have been used to express molecules in Purkinje cells *in vivo*. However, each vector has certain drawbacks. For example, approximately 30% of the cells infected by one of the best Purkinje cell-specific lentiviral vectors are non-Purkinje cells (Takayama *et al.*, 2008). In addition, it takes several days to weeks for AAV and lentiviral vectors to maximally express foreign genes. Finally, it is often difficult to express large and multiple genes in Purkinje cells with viral vectors. Therefore, a method that can complement the current transgenic and viral vector approaches is desired.

In utero electroporation (IUE), in which electrical pulses are applied through the uterine wall, has recently emerged as a useful method for transferring genes into restricted types of neuronal precursors *in vivo* (Saito & Nakatsuji, 2001; Tabata & Nakajima, 2001). An advantage of IUE is that large and multiple genes can be introduced into neurons during very early developmental periods (De Vry *et al.*, 2010). Furthermore, by using cell-type-specific and/or inducible promoters, foreign genes can be expressed in a particular neuronal subset within a distinct time frame (Kolk *et al.*, 2011). Although IUE has been successfully applied to various neurons in the cerebral cortex (Saito & Nakatsuji, 2001; Tabata & Nakajima, 2001), hippocampus (Navarro-Quiroga *et al.*, 2007), thalamus (Bonnin *et al.*, 2007) and cerebellum (Kawauchi *et al.*, 2006; Kawauchi & Saito, 2008; Tamada *et al.*, 2008), Purkinje cells have not been transfected. Here, we report a new IUE method for the selective, effective and temporally regulated expression of multiple foreign genes in Purkinje cells *in vivo*. We also show that IUE did not alter the physiological characteristics or normal synaptic plasticity of the Purkinje cells.

Materials and methods

Experimental mice were killed by decapitation after anesthetization with tribromoethanol. All animal care and treatment procedures were performed in accordance with the NIH guidelines and approved by the Animal Resource Committee of the School of Medicine, Keio University.

cDNA constructs

pCAG-ER^{T2}CreER^{T2} and pCALNL-DsRed2 (Matsuda & Cepko, 2007) were kindly provided by Dr T. Matsuda (Kyoto University, Kyoto, Japan). The fragment encoding enhanced green fluorescent protein (EGFP) of pBSII-L7-EGFP (Oberdick *et al.*, 1990; Tomomura *et al.*, 2001) was replaced with the ER^{T2}CreER^{T2} fragment of pCAG-ER^{T2}CreER^{T2}, and the L7-ER^{T2}CreER^{T2} fragment was then subcloned into the pCL20 vector (Torashima *et al.*, 2006). pCAG-EGFP-β-actin (Furuyashiki *et al.*, 2002) was a kind gift from Dr H. Bito (University of Tokyo, Tokyo, Japan). pCMV-Mito-ECFP, which encodes enhanced cyan fluorescent protein (ECFP) fused with a mitochondrial targeting sequence derived from the subunit VIII of human cytochrome C oxidase, was obtained from Clontech (Mountain View, CA, USA). Mito-ECFP was subcloned into the pCAGGS vector (kindly provided by Dr J. Miyazaki, Osaka University, Osaka, Japan). The full-length cDNA clone encoding mouse retinoid-related orphan receptor α1 (RORα1) was isolated by PCR from the total RNA of mouse cerebellum. The following primer set was used: 5′-ATG GAGTCAGCTCCGGC-3′ and 5′-TTACCCATCGATTTGCATGG-3′. The nucleotide sequence of the amplified open reading frame was confirmed using bidirectional sequencing. To produce a dominant-negative form of RORα1, cDNA encoding a hemagglutinin (HA) tag was added to the 3′ end of the cDNA fragment encoding amino acids 1–235 of RORα1 (RORα1DN-HA). The resultant cDNA was subcloned into the pCAGGS vector to generate pCAG-RORα1DN-HA. The plasmid encoding EGFP-Bassoon was kindly provided by Dr T. Ohtsuka (University of Yamanashi, Yamanashi, Japan). The fragment encoding EGFP was replaced with that of mCherry and the mCherry-Bassoon fragment was subcloned into the pCAGGS vector.

In utero electroporation

Pregnant ICR mice at embryonic day (E)11.5 or E12.5 (SLC, Shizuoka, Japan) were deeply anesthetized via an intraperitoneal injection (50–60 μg/g) of sodium pentobarbital (Somnopentil; Kyoritsu Seiyaku Co., Tokyo, Japan). To relax the myometrium, ritodorin hydrochloride (1–1.4 μg/g; Sigma-Aldrich, St Louis, MO, USA) was applied to the exposed uterine horns. Plasmid DNAs, purified using the Qiagen plasmid maxi kit (Hilden, Germany), were dissolved in HEPES-buffered saline at a final concentration of 1–5 mg/mL (1–2 mg/mL for introducing CAG-EGFP alone and 5 mg/mL for introducing CALNL-DsRed2, L7-ERT2CreERT2 and CAG-EGFP (at a ratio of 3 : 2 : 1)] together with Fast Green (final concentration 0.01%). The plasmid solution (1–3 μL) was injected by air pressure into the fourth ventricle using a mouth-controlled micropipette or microinjector (Microinjector 5242; Eppendorf, Hamburg, Germany) under the illumination of a fiber optic light source. The embryo was held through the uterus with tweezers-type electrodes (CUY650P3; NEPA Gene, Chiba, Japan), and electrical pulses (33 V, with a duration of 30 ms, at intervals of 970 ms per pulse) were delivered five times with an electroporater (CUY21SC; NEPA Gene). In some experiments, two series of pulses were applied to deliver genes into the bilateral cerebellum. After electroporation, the uterus was repositioned in the abdominal cavity, the abdominal wall and skin were closed, and the embryos were allowed to continue developing normally.

Electrophysiology

Acute cerebellar slices (200 μm thick in sagittal section) were prepared from the electroporated ICR mice at postnatal day (P)25–28, and whole-cell patch-clamp recordings were performed from visually identified Purkinje cells that emitted EGFP fluorescence, as described previously (Kakegawa *et al.*, 2009). The resistance of the patch pipettes was 3–5 MΩ when filled with the following internal solution (in mM): 65 Cs-methanesulfonate, 65 K-gluconate, 20 HEPES, 10 KCl, 1 MgCl$_2$, 4 Na$_2$ATP, 1 Na$_2$GTP, 5 sucrose and 0.4 EGTA, pH 7.25 (295 mOsm/kg). For slice storage and recording, the following solution was used (in mM): 125 NaCl, 2.5 KCl, 2 CaCl$_2$, 1 MgCl$_2$, 1.25 NaH$_2$PO$_4$, 26 NaHCO$_3$ and 10 D-glucose. This solution was bubbled continuously with a mixture of 95% O$_2$ and 5% CO$_2$ at room temperature. Picrotoxin (100 μM; Sigma) was always present in the saline to block inhibitory synaptic transmission. To elicit PF-evoked and climbing fiber (CF)-evoked excitatory postsynaptic currents (EPSCs), a stimulating glass pipette was placed on the molecular layer and granular layer, respectively (square pulse, 10 μs, ~200 μA). Selective stimulations of each fiber type were confirmed by the paired-pulse facilitation for PF–EPSC and paired-pulse depression for CF–EPSC with a 50-ms stimulation interval.

In the LTD sessions, PF–EPSCs were recorded successively at a frequency of 0.1 Hz from Purkinje cells clamped at −80 mV (Kakegawa *et al.*, 2009). After stable PF–EPSCs were observed for at least 10 min, a conjunctive stimulation (CJ-stim), consisting of 30 single PF stimuli together with a 200-ms depolarizing pulse from a holding potential of −60 to +20 mV, was applied to induce LTD. Access resistances were monitored every 10 s by measuring the peak currents in response to hyperpolarizing steps (50 ms, 2 mV) throughout the experiments; the measurements were discarded if the resistance changed by >20% of its original value. The normalized EPSC amplitude on the ordinate represents the EPSC amplitude for the average of six traces for 1 min divided by that of the average of six traces for 1 min immediately before CJ-stim. Current responses were recorded using an Axopatch 200B amplifier (Molecular Devices, Sunnyvale, CA, USA) and the PCLAMP software (version 9.2; Molecular Devices). Signals were filtered at 1 kHz and digitized at 4 kHz.

4OHT administration

4-Hydroxytamoxifen (4OHT; Sigma) was dissolved in ethanol at a concentration of 20 mg/mL and diluted with 9 volumes of corn oil (Sigma). The diluted 4OHT (200 μL per mouse) was intraperitoneally injected into mice at P6.

Immunohistochemistry

Under deep anesthesia, the mice were fixed by cardiac perfusion with 0.1 M sodium phosphate buffer (PB), pH 7.4, containing 4% paraformaldehyde (4% PFA/PB); the cerebellum was then removed and soaked in 4% PFA/PB for 4–24 h. After rinsing the specimens with PBS, parasagittal slices (50–100 μm thick) were prepared using a microslicer (DTK-2000; Dosaka, Kyoto, Japan) and subjected to immunohistochemical staining with the following antibodies: guinea pig anti-calbindin (1 mg/mL; Nakagawa *et al.*, 1998), rabbit anti-calbindin (1 : 500; Millipore, Bedford, MA, USA), mouse anti-NF-H (1 : 1000; Covance, Berkeley, CA, USA), guinea pig anti-glial fibrillary acidic protein (GFAP; 1 mg/mL, provided by Dr Watanabe at Hokkaido University), guinea pig anti-vesicular glutamate transporter VGluT1 (1 μg/mL; Miyazaki *et al.*, 2003), mouse anti-HA (1 : 500; Covance) and goat anti-RORα (1 : 500; Santa Cruz Biotechnology, Santa Cruz, CA, USA). Sections were permeabilized with 0.1 or 0.2% Triton X-100 in PBS, blocked with 10% donkey serum in PBS, and incubated overnight with primary antibodies followed by 1–2 h of incubation with Alexa Fluor- (Invitrogen, Carlsbad, CA, USA) or DyLight- (Jackson Immunoresearch Laboratory, West Grove, PA, USA) conjugated secondary antibodies. For fluorescence Nissl staining, the sections were incubated with NeuroTrace Red (1 : 100; Invitrogen) for 1 h. The stained slices were viewed using a confocal laser-scanning microscope (Fluoview; Olympus, Tokyo, Japan or LSM710; Carl Zeiss, Göttingen, Germany).

Image analysis and statistics

To determine the cell-type specificity, parasagittal slices of cerebellar vermis (50 or 100 μm thick) were immunostained for calbindin, and the numbers of EGFP-positive cells that were calbindin-immunopositive or -immunonegative in the cerebellum were counted. Statistical significance was defined by the χ^2 test with Bonferroni correction.

To separate the emission fluorescence of Mito-ECFP, EGFP-β-actin and DsRed2, z-stack images of spectral data were obtained from a cerebellar slice by confocal microscopy (LSM710; Carl Zeiss). The images were processed by a linear unmixing algorithm (Zimmermann *et al.*, 2003) to generate three-fluorescence images. The reference spectral data were obtained from human embryonic kidney 293 cells expressing only one of the three fluorescent proteins (Mito-ECFP, EGFP-β-actin and DsRed2).

To study the effect of RORα1DN-HA on Purkinje cell development, parasagittal slices of cerebellar vermis (100 μm thick) were immunostained for calbindin and HA. The morphology of the calbindin-immunopositive and EGFP-positive Purkinje cells in the bank region of lobule III and IV/V was analysed. An EGFP-positive Purkinje cell whose soma was located at a distance more than one soma away from the Purkinje cell layer, defined by the rest of the EGFP-negative Purkinje cells, was counted as 'mislocalized'. Statistical significance was defined by the χ^2 test.

For the statistical analysis of electrophysiological results, the Mann–Whitney *U*-test was applied.

Results

Predominant expression of EGFP in Purkinje cells by IUE

Previous studies demonstrated that mouse Purkinje cells arise from the ventricular zone facing the fourth ventricle around E10–E13 (Miale & Sidman, 1961; Wang & Zoghbi, 2001; Hashimoto & Mikoshiba, 2003). Thus, to develop an IUE method for Purkinje cells, a plasmid encoding EGFP under the control of the CAG promoter (CAG-EGFP) was injected into the fourth ventricle of E10.5, E11.5 or E12.5 mice. To transfect Purkinje cell precursors, the electrodes were placed diagonally across the fourth ventricle with the anode above the cerebellar primordium at an angle of 90° or more to the targeted side of the upper rhombic lip (Fig. 1A and Supporting Information, Fig. S1), and 33-V electrical pulses were applied five times (Fig. 1A). We observed bright EGFP signals through the skin and the skull in newborn mice that had undergone IUE at E10.5, E11.5 or E12.5. The EGFP signals were observed on the electroporated side of the cerebellum (Fig. 1B, left and middle panels), but when a series of pulses was sequentially applied in two diagonal directions, both sides of the cerebellum were transfected (Fig. 1B, right panel). More EGFP-positive cells were observed in mice that underwent IUE at E11.5 than at E10.5 or E12.5 (Fig. 1B). EGFP was expressed in almost the entire half of the cerebellum that underwent IUE at E11.5 (Fig. 1B). In contrast, EGFP expression was not observed in the middle of the vermis and the edge of the hemisphere of the cerebellum that underwent IUE at E10.5; EGFP signals were restricted in the middle of the vermis and the edge of the hemisphere when IUE was performed at E12.5 (Fig. 1B). Similarly, adenovirus vectors injected into the fourth ventricle at E10.5, E11.5 and E12.5 infect only the subpopulation of Purkinje cell progenitors that were born on the day of each injection (Hashimoto & Mikoshiba, 2003). Thus, it is likely that only cells that were located at the surface of the fourth ventricle at the time of IUE were transfected.

To determine the cellular specificity of transfection, we fixed the cerebella at P14 and later and immunostained them for calbindin, a Purkinje cell marker. Again, more EGFP-positive cells were observed in the cerebellar sections taken from mice that underwent IUE at E11.5 than at E10.5 or E12.5 (Fig. 1C). The vast majority of EGFP-positive cells were immunopositive for calbindin in the cerebellum (Fig. 1C). The proportions of calbindin-immunopositive Purkinje cells in EGFP-positive cells were 99 ± 1, 96 ± 4 and 86 ± 1%, for the cerebellum that underwent IUE at E10.5, E11.5 and E12.5, respectively (Fig. 1D). Thus, Purkinje cells were more specifically transfected when IUE was performed at earlier time points ($P < 0.05$ for E10.5 vs. E11.5, $P < 0.0001$ for E11.5 vs. E12.5 and E12.5 vs. E10.5, χ^2 test with Bonferroni correction). These results indicate that when IUE was performed in a spatially directed manner by adjusting the position of the electrode and optimizing the orientation of the electrical field at E10.5–E12.5, exogenous genes could be efficiently and preferentially introduced into Purkinje cells *in vivo*.

We occasionally observed a small number of EGFP-positive, calbindin-negative neurons in the granular layer that morphologically corresponded to Golgi cells (Fig. S2A). Golgi cells and Purkinje cells arise from the ventricular zone at distinct but overlapping developmental stages in mice (Miale & Sidman, 1961; Wang & Zoghbi, 2001; Hashimoto & Mikoshiba, 2003). On very rare occasions, we observed EGFP-positive puncta in the granular layer of cerebella that underwent IUE at E12.5 (Fig. S2B and a). These puncta were immunopositive for a neuronal marker, neurofilament (Fig. S2B and b), negative for Nissl staining (Fig. S2B and c), immunonegative for a glial marker, GFAP (Fig. S2B and d), and immunopositive for vesicular glutamate transporter 1, a marker for glutamatergic nerve terminals (Fig. S2B and e).
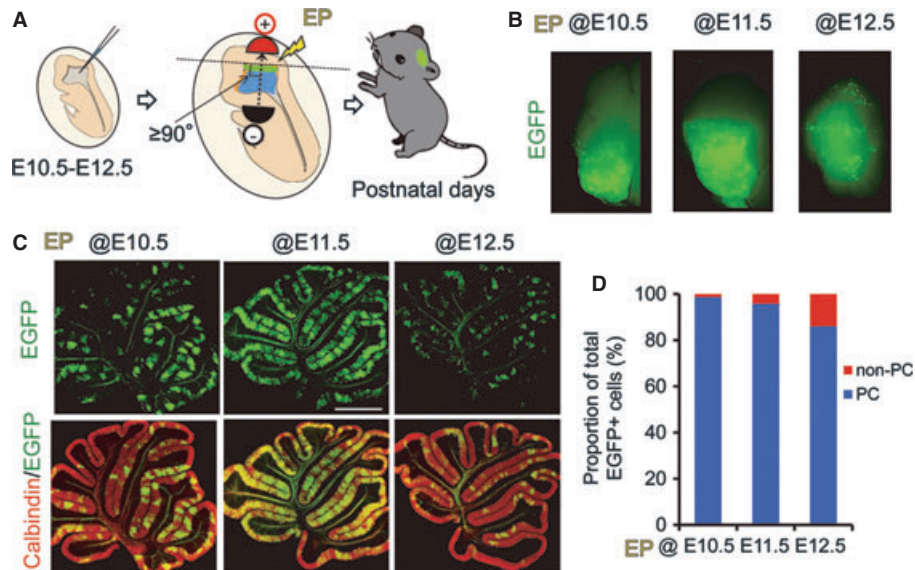
FIG. 1. Successful gene delivery into cerebellar Purkinje cells *in vivo* by IUE. (A) Schematic illustration of the procedure for IUE into Purkinje cells. A solution containing plasmid vectors was injected into the fourth ventricle, and electrical pulses were then applied unilaterally or bilaterally. To achieve efficient transfection into Purkinje cells, the angle formed by electrode and the targeted rhombic side (green) should be 90° or more (see Methods and Fig. S1). (B–C) EGFP expression in Purkinje cells by IUE. A pCAG-EGFP plasmid was electroporated at E10.5, E11.5 and E12.5. (B) The expression patterns of EGFP in the whole cerebellum at P26 (E10.5), P21 (E11.5) or P33 (E12.5) are shown. The right side of the cerebellum (E10.5 and E11.5, left and middle panels) or both sides (E12.5, right panel) were electroporated. (C) The mice were fixed at P14 and the parasagittal sections of the cerebella were immunostained for calbindin. More EGFP-positive cells in the cerebellum were observed in mice that underwent IUE at E11.5 than at E10.5 and E12.5. (D) Preferential expression of EGFP in Purkinje cells. The percentage of EGFP-positive (EGFP$^+$) cells that were calbindin-immunopositive (PCs) and calbindin-immunonegative (non-PCs) was quantified in parasagittal sections of the vermis from mice that had undergone IUE at E10.5, E11.5 and E12.5. IUE at earlier time points more preferentially transfected Purkinje cells. $n = 451$ (E10.5), 1235 (E11.5) and 407 (E12.5) cells from two (E10.5) or three (E11.5 and E12.5) independent experiments. Scale bar, 1 mm.

These results indicate that, depending on subtle differences in the diagonal angle of the electrodes, plasmids could also be incorporated into precerebellar nuclei neurons, which are generated in the caudal rhombic lip at around E12.5, which expressed EGFP in mossy fibers. In addition, we observed a small number of EGFP-positive neurons in the deep cerebellar nucleus (Fig. S3A), which are produced in the rostal rhombic lip around E11.5 (Miale & Sidman, 1961). Outside the cerebellum, we occasionally observed EGFP-positive cells in the parabrachial nucleus and dorsal cochlear nucleus (Fig. 3D and S3B), which are produced in the caudal rhombic lip between E10 and 12.5 (Wang, 2005, Pierce, 1967). As EGFP positive cells in the dorsal cochlear nucleus were immunopositive for carbonic anhydrase related protein 8 (Fig. S3B), they probably correspond to cartwheel cells in the dorsal cochlear nucleus. Nevertheless, in all cases in which the spatially directed IUE was carried out at E11.5, the vast majority of transfected cells were calbindin-positive Purkinje cells.

Electrophysiological analysis of the Purkinje cells that express EGFP after IUE

Purkinje cells are particularly vulnerable cerebellar neurons (Slemmer *et al.*, 2005). Thus, to ensure that the repetitive voltage pulses during IUE (De Vry *et al.*, 2010) did not alter the developmental profile and physiological characteristics of the Purkinje cells, we performed IUE at E11.5 and examined the functional properties of the Purkinje cells at P25–P28. Confocal microscopy of fixed parasagittal sections of the vermis showed that the electroporated Purkinje cells appeared grossly normal, with elaborate dendrites and spines (Fig. 2A).

Whole-cell patch-clamp recordings showed that the input resistance and membrane capacitance of the EGFP-positive Purkinje cells from mice that underwent IUE at E11.5 were similar to those of wild-type

Purkinje cells (Table 1). In addition, there were no significant differences in either the PF– or CF–EPSC kinetics (Table 1). The PF– and CF–EPSCs in the EGFP-positive Purkinje cells showed the typical paired-pulse facilitation and paired-pulse depression, respectively, that were observed in wild-type Purkinje cells (Fig. 2B and Table 1).

By the end of the third postnatal week in mice, most wild-type Purkinje cells lose their redundant CFs and become innervated by a single CF. EGFP-positive Purkinje cells electroporated at E11.5 were similarly innervated by a single CF, as shown by their single threshold for excitation (Fig. 2C). Furthermore, the input–output relationships of the PF–EPSC were not significantly different between the electroporated EGFP-positive and wild-type Purkinje cells (Fig. 2D), indicating that the PF inputs to Purkinje cells were also intact. Finally, the conjunctive stimulation of PFs and the depolarization of Purkinje cells induced LTD similarly in both wild-type and electroporated Purkinje cells (Fig. 2E; $67 \pm 5\%$ at $t = 25$–30 min, $n = 7$ from four wild-type mice; $69 \pm 6\%$ at $t = 25$–30 min, $n = 7$ from four electroporated Purkinje cells; Mann–Whitney U-test, $P = 0.947$). Together, these results indicate that IUE did not alter the basic membrane properties, EPSC parameters, or short-term or long-term synaptic plasticity of the transfected Purkinje cells.

Temporal and Purkinje cell-specific expression of transgenes by IUE

To examine whether cell-type-specific and inducible promoters were compatible with the IUE method for Purkinje cells, we employed an inducible Cre/loxP system (Matsuda & Cepko, 2007). The Purkinje-specific L7 promoter (Oberdick *et al.*, 1990; Smeyne *et al.*, 1991; Tomomura *et al.*, 2001) was used to express the conditionally active form of Cre recombinase ER^{T2}CreER^{T2}, in which the ligand-binding
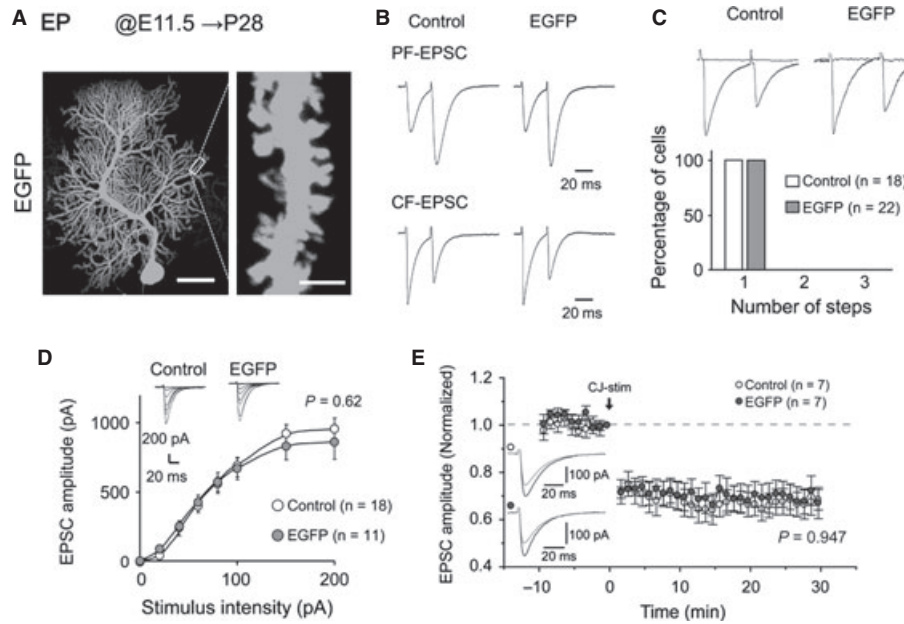
FIG. 2. Normal physiological characteristics of Purkinje cells transfected by IUE. (A) Representative images of Purkinje cells transfected with pCAG-EGFP by IUE electroporated at E11.5. At P28, parasagittal sections of the cerebella were fixed. The right panel shows a magnified image of a dendrite with elaborate spines. Scale bars, 30 μm (left) and 2 μm (right). (B) Representative PF–EPSCs (upper) and CF–EPSCs (lower) recorded from wild-type (left) and electroporated EGFP-positive (right) Purkinje cells. The inter-stimulus interval was 50 ms. (C) Histogram showing the number of CF innervation patterns between wild-type (open column, $n = 18$) and electroporated EGFP-positive (green column, $n = 22$) Purkinje cells in adult mice. Inset traces show CF–EPSCs recorded from both groups with altered stimulus intensity. (D) Input–output curves of PF–EPSC amplitude between wild-type (open circles, $n = 18$) and electroporated EGFP-positive (green circles, $n = 11$) Purkinje cells. (E) LTD data recorded from wild-type (open circles, $n = 7$) and electroporated EGFP-positive (green circles, $n = 7$) Purkinje cells. Insets show PF–EPSC traces recorded from each type of cell just before (black traces) and 30 min after (gray traces) CJ-stim (arrow). Error bars indicate SEM.

TABLE 1. Basic electrophysiological properties of Purkinje cells transfected by IUE*

	Wild-type (Control)	Electroporated (EGFP)
Membrane properties		
Membrane capacitance (pF)	1033 ± 36 ($n = 14$)	932 ± 45 ($n = 21$)
Input resistance (MΩ)	64.3 ± 3.4 ($n = 14$)	68.5 ± 6.7 ($n = 21$)
PF–EPSC		
10–90% rise time (ms)	3.29 ± 0.14 ($n = 16$)	3.29 ± 0.15 ($n = 21$)
Decay time constant (ms)	31.2 ± 0.6 ($n = 16$)	28.4 ± 1.5 ($n = 21$)
Paired-pulse ratio	1.77 ± 0.07 ($n = 16$)	1.86 ± 0.05 ($n = 31$)
CF–EPSC		
10–90% rise time (ms)	0.89 ± 0.05 ($n = 16$)	0.84 ± 0.04 ($n = 21$)
Decay time constant (ms)	19.6 ± 1.4 ($n = 16$)	19.2 ± 2.0 ($n = 21$)
Paired-pulse ratio	0.71 ± 0.02 ($n = 16$)	0.73 ± 0.01 ($n = 21$)

*There were no significant differences in each parameter ($P > 0.2$).

domain of the estrogen receptor was mutated; the Cre recombinase is activated in response to 4OHT (Matsuda & Cepko, 2007). By coexpressing pCALNL-DsRed2, which contains the CAG promoter and a stop signal flanked by loxP sequences, the reporter gene DsRed2 was designed to be expressed in a 4OHT/Cre- and L7-dependent manner (Fig. 3A). To unconditionally label all the electroporated cells, pCAG-EGFP was co-electroporated with the pL7-ER^{T2}CreER^{T2} and pCALNL-DsRed2. After IUE at E11.5, the mice received an intraperitoneal injection of 4OHT or vehicle at P6 and were fixed at P14 (Fig. 3A).

As expected, only mice that received 4OHT displayed DsRed2 signals in the cerebellum (Fig. 3B). Confocal microscopy further confirmed that the DsRed2 signals were observed only in a subset of

EGFP-positive Purkinje cells (Fig. 3C). Why some Purkinje cells escaped recombination is unclear, but ER^{T2}CreER^{T2} may have less activity than the original Cre recombinase because of the fusion with the two ER^{T2} cassettes and its altered degradation pathway (Matsuda & Cepko, 2007). Although a very small number of non-Purkinje cells were sometimes EGFP-positive, they were always negative for DsRed2 (Fig. 3D, a–c). The only DsRed2 signals observed outside the cerebellum were within the dorsal cochlear nucleus (Fig. 3D, d). Indeed, cartwheel cells in the dorsal cochlear nucleus are known to share several cell markers, such as calbindin and L7, with Purkinje cells, and cartwheel and Purkinje cells are probably derived from common precursors (Berrebi *et al.*, 1990). Together, these results indicate that IUE can drive the expression of exogenous genes specifically in Purkinje cells in a temporally controlled manner, by using the L7 promoter and inducible Cre/loxP system.

As shown by the successful application of an inducible Cre/loxP system consisting of three plasmids (Fig. 3A), a major advantage of the gene delivery by *in vivo* electroporation is that multiple and very large genes can be coexpressed with high efficiency (Saito & Nakatsuji, 2001; Matsuda & Cepko, 2007; Barnabe-Heider *et al.*, 2008). To further confirm this principle in our system, we electroporated at E11.5 three plasmids encoding three different fluorescent proteins: mito-ECFP, which is designed to localize to mitochondria, EGFP-β-actin (Furuya-shiki *et al.*, 2002) and DsRed2. The confocal z-stack images of spectral data were obtained on fixed sagittal sections at P14, and the individual ECFP, EGFP and DsRed2 fluorescence images were separated by the linear unmixing method (Zimmermann *et al.*, 2003). Most labeled Purkinje cells (99.1%; 445 of 449 cells) expressed all three fluorescent proteins (Fig. 4). The DsRed2 signals were observed diffusely throughout Purkinje cells, including the soma, dendrites, spines and axons. In contrast, the EGFP-β-actin signals accumulated in the
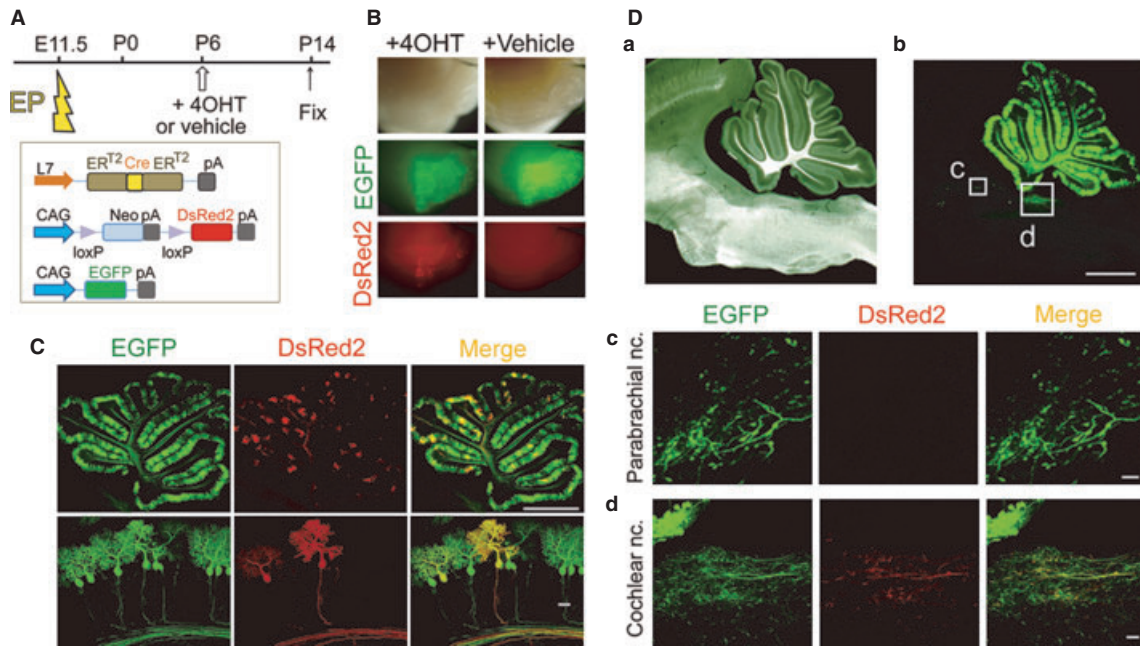
FIG. 3. Temporal and Purkinje cell-specific expression of transgenes by IUE. (A) Schematic diagram of the experimental design. Three plasmids were electroporated at E11.5: pL7-ER^{T2}CreER^{T2}, which encodes Cre recombinase flanked by a mutated estrogen receptor (ER^{T2}) under the control of a Purkinje-cell-specific promoter L7; pCALNL-DsRed2, which contains the CAG promoter and a stop signal flanked by loxP sequences; and pCAG-EGFP, which expresses EGFP under the CAG promoter (at a ratio of 2 : 3 : 1). 4OHT was injected intraperitoneally at P6, and the mice were fixed at P14. (B) Representative images of EGFP and DsRed2 signals in the cerebellum at P14. DsRed2 signals were specifically observed in the cerebellum from mice treated with 4OHT (left) but not in those treated with vehicle alone (right). (C) Confocal images of parasagittal sections of the cerebellum from mice treated with 4OHT. DsRed2 signals were observed in a subpopulation of EGFP-positive Purkinje cells. Scale bars, 1 mm (upper) and 30 μm (lower). (D) L7-driven Cre enabled the specific expression of transgenes in Purkinje cells. The vast majority of EGFP signals were confined to the cerebellum (a, bright field; b, EGFP signals). EGFP-positive cells were sometimes observed in the brainstem (the parabrachial nucleus is shown as a box in b and enlarged in c). The dorsal cochlear nucleus (shown as a box in b and enlarged in d) contained EGFP and DsRed2 double-positive cells, which share common progenitors with Purkinje cells. Scale bars, 1 mm (b) and 30 μm (c, d).

dendritic spines and nuclei, while the mito-ECFP signals were observed in the soma and dendritic shafts. Next, to examine whether a large gene can be introduced into Purkinje cells by IUE, we used cDNA encoding Bassoon, a large protein selectively localized at the active zone of presynaptic nerve terminals (tom Dieck *et al.*, 1998). We electroporated a plasmid (approximately 17 kb) encoding mouse Bassoon fused to mCherry (mCherry-Bassoon; approximately 12.5 kb) and a plasmid encoding EGFP at E11.5. Confocal imaging of fixed cerebellum at P14 revealed punctate mCherry-Bassoon signals along EGFP-positive Purkinje cell axons (Fig. S4). In addition, mCherry-Bassoon signals were colocalized with immunoreactivity for vesicular GABA transporter (VGAT), a presynaptic marker (Fig. S4). Together, these results illustrate that an advantage of IUE-based gene delivery into Purkinje cells is that not only can multiple genes be coexpressed, but also that large genes can be transfected with high efficiency.

Molecular perturbation of Purkinje cell development by IUE

Another advantage of IUE is that exogenous genes can be introduced into restricted types of neuronal progenitors, facilitating the study of early developmental events in postmitotic neurons in various brain regions (De Vry *et al.*, 2010). To confirm that this advantage applies to Purkinje cells, we sought to molecularly perturb their early developmental processes by IUE. The ataxic mouse mutant *staggerer* is caused by a deletion in the gene encoding RORα1 (Sidman *et al.*, 1962; Hamilton *et al.*, 1996). As RORα1 lacking the putative ligand-binding domain (RORα1DN) serves as a dominant-negative mutant in cultured muscle cells (Lau *et al.*, 1999, 2004) (Fig. 5A), we introduced two plasmids, pCAG-RORα1DN-HA, in which HA-tagged

RORα1DN was placed under the CAG promoter, and pCAG-EGFP, into Purkinje cells by IUE at E11.5.

The mice were fixed at P9, and sagittal sections at the vermis were immunostained for calbindin and HA to visualize Purkinje cells and RORα1DN, respectively. Confocal microscopy showed that almost all the control calbindin-positive Purkinje cells expressing EGFP had single primary dendrites (96.2%, 102 of 106 cells; Fig. 5B and C). By contrast, only half of the calbindin-positive Purkinje cells expressing EGFP and RORα1DN-HA had a single primary dendrite (49.5%, 50 of 101 cells; $P < 0.0001$ vs. control, χ^2 test), and the remaining cells had from two to five primitive dendrites (Fig. 5B and C). Furthermore, while all the control Purkinje cells expressing EGFP were arranged in a monolayer together with non-transfected Purkinje cells, a small number of Purkinje cells expressing RORα1DN-HA (six of 101) were mislocalized to the granular layer (Fig. 5B, arrowheads). These phenotypes observed in Purkinje cells expressing RORα1DN-HA were reminiscent of those observed in *staggerer* Purkinje cells (Soha & Herrup, 1995; Nakagawa *et al.*, 1998). These results clearly indicate that certain *staggerer* phenotypes can be mimicked by the IUE-mediated expression of dominant-negative RORα1 in single Purkinje cells during early development.

Discussion

Although IUE has several advantages as a method for transferring genes into neurons *in vivo*, it has never been applied to cerebellar Purkinje cells, key neurons for regulating cerebellar functions. In the present study, we showed that Purkinje cell progenitors at E11.5 could be most efficiently and preferentially transfected by IUE, by properly
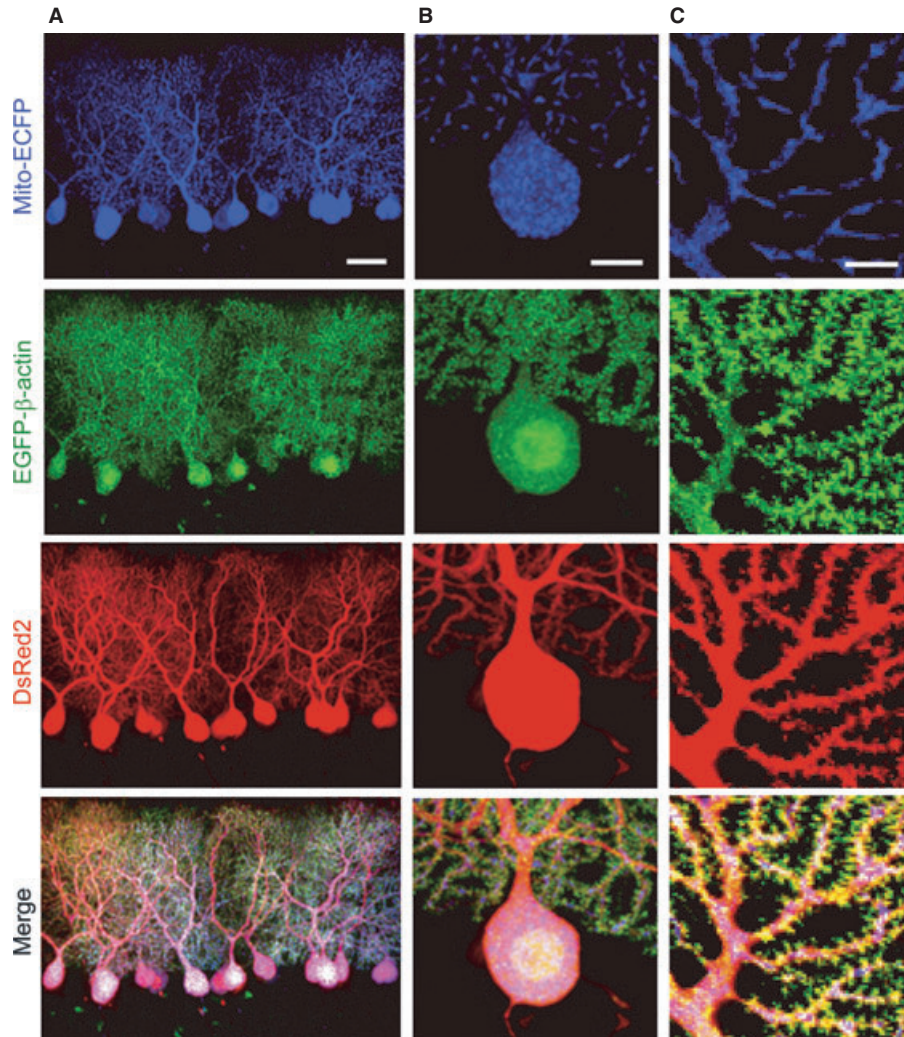
FIG. 4. Efficient co-expression of three plasmids encoding different fluorescent proteins. An E11.5 mouse embryo was co-electroporated with three plasmids encoding different fluorescent proteins: pCAG-DsRed2, pCAG-Mito-ECFP and pCAG-EGFP-β-actin, at a ratio of 1 : 2 : 2. At P14, parasagittal cerebellar sections were analysed using confocal laser scanning microscopy. The confocal z-stack images of spectra data were obtained, and the individual ECFP, EGFP and DsRed2 fluorescence images were separated by the linear unmixing method. The three different fluorescent proteins were simultaneously coexpressed in Purkinje cells with distinct expression patterns. Scale bars, 30 μm (A); 10 μm (B); 5 μm (C).

adjusting the angle and direction of the electrodes (Fig. 1). Electro-physiological analyses indicated that the electroporated Purkinje cells maintained normal membrane properties, synaptic responses and synaptic plasticity at P28 (Fig. 2). We also showed that simultaneous expression of three different fluorescent proteins (Fig. 4) and expression of a large gene (Bassoon; Fig. S4) could be successfully achieved by IUE in Purkinje cells. In addition, by using three plasmids encoding the L7 promoter and an inducible Cre∕Lox system, we could achieve temporal and Purkinje-cell-specific transgene expression (Fig. 3). These results show that this new IUE protocol enables the selective and regulated expression of multiple foreign genes in Purkinje cell progenitors without deleterious effects.

As an alternative approach to genetic manipulation of mice, considerable effort has been devoted to transduce Purkinje cells using various types of viral vectors (Hirai, 2008). However, each vector has limitations with respect to the efficiency, specificity, toxicity and length of the insert. For example, AAV vectors have strict limitation of the length of insert up to 5 kb including a promoter (Wu *et al.*, 2010). The limit for the length of insert for lentiviral vectors is up to 8 kb (Hirai, 2008). In addition, 30% of cells infected by one of the best

Purkinje cell-specific lentiviral vectors were non-Purkinje cells, such as Bergmann glia, stellate and basket cells (Takayama *et al.*, 2008). The Sindbis virus enables the rapid production of high levels of recombinant protein in Purkinje cells; however, its use is limited by the cytotoxicity to Purkinje cells (Kohda *et al.*, 2007). The adenovirus vectors preferentially infect Bergmann glia rather than Purkinje cells *in vivo* (Hashimoto *et al.*, 1996; Terashima *et al.*, 1997; Kakegawa *et al.*, 2011). Although injection of adenovirus into the fourth ventricle of embryonic mice could efficiently deliver genes into cerebellar progenitors (Hashimoto & Mikoshiba, 2003), cell-type specificity was not examined at the cellular level. It also remains unclear whether Purkinje cells infected with adenovirus *in utero* maintain normal physiological properties, such as synaptic plasticity. Therefore, we believe that the new IUE protocol can complement the current transgenic and viral vector approaches; major advantages of IUE include simplicity, high specificity to Purkinje cells, low toxicity, and high efficiency to introduce large and multiple genes.

A drawback of the current IUE protocol is that although Purkinje cells are always transfected, a small number of neurons, which are probably generated near the rhombic lip during a similar time window,
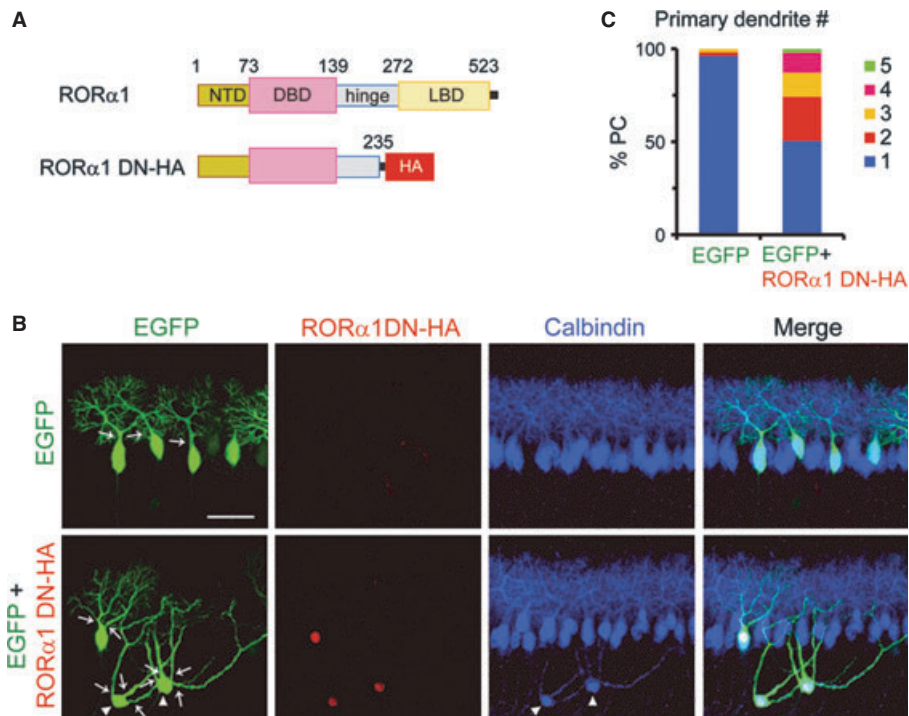
FIG. 5. *Staggerer*-like phenotypes recapitulated by the IUE-mediated expression of a dominant-negative form of RORα1 in Purkinje cells. (A) Schematic diagram of the functional domains of the wild-type and dominant-negative RORα1 proteins. Wild-type RORα1 consists of four major functional domains: an *N*-terminal domain (NTD) followed by a DNA-binding domain (DBD), a hinge domain and a *C*-terminal ligand-binding domain (LBD). A hemagglutinin (HA) tag was added just after amino acid 235 to create a dominant-negative form (RORα1DN-HA). Amino acid numbers are indicated above the wild-type RORα1. (B) Representative images of Purkinje cells overexpressing EGFP only (upper panels) or EGFP and RORα1DN-HA (lower panels). Mice were electroporated at E11.5 with pCAG-EGFP (control), or with pCAG-EGFP plus pCAG-RORα1DN-HA (mixed at a ratio of 1 : 3). At P9, the mice were fixed, and parasagittal cerebellar sections were immunostained for HA-tag (red) and calbindin (blue). Arrows indicate primary dendrites, and arrowheads indicate calbindin-positive cell bodies mislocalized to the granular layer. (C) Quantitative analyses of the number of primary dendrites of Purkinje cells. While almost all of the control P9 Purkinje cells had a single primary dendrite, Purkinje cells expressing RORα1DN-HA often had multiple primary dendrites. $n = 106$ cells (control) and $n = 101$ cells (RORα1DN-HA) from two independent experiments for each condition. Scale bar, 50 μm.

are sometimes transfected as well. Although cell specificity can be easily achieved by using the L7 promoter (Fig. 3), early expression of a transgene is then limited by the L7 promoter activity. Nevertheless, as a method for transferring genes into Purkinje cells, IUE has a better specificity for Purkinje cells than lentivirus vectors (Fig. 1D; Torashima *et al.*, 2006).

Another drawback of the IUE method is that it can only introduce genes in a subpopulation of Purkinje cells. This is partly because only the Purkinje cell progenitors that are located at the surface of the fourth ventricle at the time of IUE will be transfected. Similarly, adenovirus vectors injected into the fourth ventricle at E11.5 and E12.5 infect only the subpopulation of Purkinje cell progenitors that were born on the day of each injection (Hashimoto *et al.*, 1996). However, close observation revealed that unlike distinct mediolateral clusters labeled by the adenovirus vector, clusters labeled by IUE at different embryonic days showed a certain overlap between each other (Fig. 1B). This could be caused by the use of different reporter genes (nuclear-targeted β-galactosidase in the previous study vs. cytosolic EGFP in the current study) and the different mechanism by which genes were delivered to neurons. The efficiency of DNA entry into cells is also compromised in the IUE method, as a trade-off in preventing electroporation-induced damage to the embryo. Nevertheless, we found that transfected Purkinje cells could efficiently coexpress at least three transgenes (Figs 3 and 4). This situation is quite advantageous for electrophysiological analyses, because recordings from transfected and

neighboring non-transfected (control) neurons can be easily compared. In addition, EGFP introduced at E11.5 remained highly expressed 1 month after birth (Fig. 2) and was maintained at least until P90 (data not shown).

Immature Purkinje cells originally have a fusiform shape with a few dendrites. Purkinje cells lose these primitive dendrites almost completely by P3–P4 in rats (Sotelo & Dusart, 2009). As the virus-mediated overexpression of human RORα1 accelerates this process in wild-type and restores it in *staggerer* cerebellum organotypic slice cultures, RORα1 was proposed to play a crucial role in the regression of primitive dendritic branches (Boukhtouche *et al.*, 2006). In the present study, we showed that the IUE-mediated overexpression of dominant-negative RORα1 in Purkinje cells *in vivo* could recapitulate the morphological abnormalities observed in *staggerer* mice (Fig. 5). These results not only support but also extend the hypothesis that cell-autonomous activities of RORα1 in Purkinje cells are responsible for the process controlling the regression of primitive dendrites *in vivo*.

Notably, because of the limited migration of Purkinje cells in organotypic slice cultures, the migration defect of *staggerer* Purkinje cells was not analysed previously (Boukhtouche *et al.*, 2006), and it remains unclear whether the regressive phase begins during or after the migration of Purkinje cells to their final domains. We observed that some Purkinje cells expressing dominant-negative RORα1 did not reach the Purkinje cell layer *in vivo*, indicating that RORα1 regulates not only the regression of dendrites but also the migration process of Purkinje cells. It is unclear why the phenotypes of Purkinje cells

expressing dominant-negative RORα1 were variable, but small differences in transgene expression levels and/or the developmental stage of the transfected Purkinje cell progenitors could have contributed to the variation. A more robust suppression of RORα1 gene expression by IUE-based RNA interference (Matsuda & Cepko, 2004) will help clarify the role of RORα1 in the early events during Purkinje-cell development.

Future studies taking advantage of IUE to enable gene expression from the early postmitotic stage will facilitate studies on the mechanisms of Purkinje cell development and migration. Furthermore, with the use of an inducible Cre/loxP system and the L7 promoter, the IUE protocol for Purkinje cells will also serve as a powerful tool for elucidating the molecular mechanisms underlying learning and memory and certain cerebellar disorders.

Supporting Information

Additional supporting information may be found in the online version of this article:

Fig. S1. Orientation of electrodes for efficient gene delivery into Purkinje cells by IUE.

Fig. S2. EGFP-positive and calbindin-negative cells and fibers in the granular layer of the cerebellum.

Fig. S3. EGFP-positive cells in the deep cerebellar nucleus and the dorsal cochlear nucleus.

Fig. S4. IUE-mediated expression of mCherry-Bassoon in Purkinje cell axons.

Please note: As a service to our authors and readers, this journal provides supporting information supplied by the authors. Such materials are peer-reviewed and may be re-organized for online delivery, but are not copy-edited or typeset by Wiley-Blackwell. Technical support issues arising from supporting information (other than missing files) should be addressed to the authors.

Acknowledgements

Abbreviations

4OHT, 4-hydroxytamoxifen; AAV, adeno-associated virus; CF, climbing fiber; CJ-stim, conjunctive stimulation; ECFP, enhanced cyan fluorescent protein; EGFP, enhanced green fluorescent protein; EPSC, excitatory postsynaptic current; HA, hemagglutinin; IUE, *in utero* electroporation; LTD, long-term depression; PB, phosphate buffer; PF, parallel fiber; PFA, paraformaldehyde; RORα1, retinoid-related orphan receptor α1; VGAT, vesicular GABA transporter.

References

Agudo, M., Trejo, J.L., Lim, F., Avila, J., Torres-Aleman, I., Diaz-Nido, J. & Wandosell, F. (2002) Highly efficient and specific gene transfer to Purkinje cells *in vivo* using a herpes simplex virus I amplicon. *Hum. Gene Ther.*, **13**, 665–674.

Altman, J. & Bayer, S.A. (1997). *Development of the Cerebellar System: in Relation to its Evolution, Structure and Functions.* CRC Press, Boca Raton, FL.

Barnabe-Heider, F., Meletis, K., Eriksson, M., Bergmann, O., Sabelstrom, H., Harvey, M.A., Mikkers, H. & Frisen, J. (2008) Genetic manipulation of adult mouse neurogenic niches by *in vivo* electroporation. *Nat. Methods*, **5**, 189–196.

Berrebi, A.S., Morgan, J.I. & Mugnaini, E. (1990) The Purkinje cell class may extend beyond the cerebellum. *J. Neurocytol.*, **19**, 643–654.

Bonnin, A., Torii, M., Wang, L., Rakic, P. & Levitt, P. (2007) Serotonin modulates the response of embryonic thalamocortical axons to netrin-1. *Nat. Neurosci.*, **10**, 588–597.

Boukhtouche, F., Doulazmi, M., Frederic, F., Dusart, I., Brugg, B. & Mariani, J. (2006) RORalpha, a pivotal nuclear receptor for Purkinje neuron survival and differentiation: from development to ageing. *Cerebellum*, **5**, 97–104.

De Vry, J., Martinez-Martinez, P., Losen, M., Temel, Y., Steckler, T., Steinbusch, H.W., De Baets, M.H. & Prickaerts, J. (2010) *In vivo* electroporation of the central nervous system: a non-viral approach for targeted gene delivery. *Prog. Neurobiol.*, **92**, 227–244.

tom Dieck, S., Sanmarti-Vila, L., Langnaese, K., Richter, K., Kindler, S., Soyke, A., Wex, H., Smalla, K.H., Kampf, U., Franzer, J.T., Stumm, M., Garner, C.C. & Gundelfinger, E.D. (1998) Bassoon, a novel zinc-finger CAG/glutamine-repeat protein selectively localized at the active zone of presynaptic nerve terminals. *J. Cell Biol.*, **142**, 499–509.

Furuyashiki, T., Arakawa, Y., Takemoto-Kimura, S., Bito, H. & Narumiya, S. (2002) Multiple spatiotemporal modes of actin reorganization by NMDA receptors and voltage-gated Ca^{2+} channels. *Proc. Natl. Acad. Sci. USA*, **99**, 14458–14463.

Hamilton, B.A., Frankel, W.N., Kerrebrock, A.W., Hawkins, T.L., FitzHugh, W., Kusumi, K., Russell, L.B., Mueller, K.L., van Berkel, V., Birren, B.W., Kruglyak, L. & Lander, E.S. (1996) Disruption of the nuclear hormone receptor RORalpha in staggerer mice. *Nature*, **379**, 736–739.

Hashimoto, M. & Mikoshiba, K. (2003) Mediolateral compartmentalization of the cerebellum is determined on the 'birth date' of Purkinje cells. *J. Neurosci.*, **23**, 11342–11351.

Hashimoto, M., Aruga, J., Hosoya, Y., Kanegae, Y., Saito, I. & Mikoshiba, K. (1996) A neural cell-type-specific expression system using recombinant adenovirus vectors. *Hum. Gene Ther.*, **7**, 149–158.

Hirai, H. (2008) Progress in transduction of cerebellar Purkinje cells *in vivo* using viral vectors. *Cerebellum*, **7**, 273–278.

Ito, M. (1989) Long-term depression. *Annu. Rev. Neurosci.*, **12**, 85–102.

Kaemmerer, W.F., Reddy, R.G., Warlick, C.A., Hartung, S.D., McIvor, R.S. & Low, W.C. (2000) *In vivo* transduction of cerebellar Purkinje cells using adeno-associated virus vectors. *Mol. Ther.*, **2**, 446–457.

Kakegawa, W., Miyazaki, T., Kohda, K., Matsuda, K., Emi, K., Motohashi, J., Watanabe, M. & Yuzaki, M. (2009) The *N*-terminal domain of GluD2 (GluRdelta2) recruits presynaptic terminals and regulates synaptogenesis in the cerebellum *in vivo*. *J. Neurosci.*, **29**, 5738–5748.

Kakegawa, W., Miyoshi, Y., Hamase, K., Matsuda, S., Matsuda, K., Kohda, K., Emi, K., Motohashi, J., Konno, R., Zaitsu, K. & Yuzaki, M. (2011) D-serine regulates cerebellar LTD and motor coordination through the delta2 glutamate receptor. *Nat. Neurosci.*, **14**, 603–611.

Kawauchi, D. & Saito, T. (2008) Transcriptional cascade from Math1 to Mbh1 and Mbh2 is required for cerebellar granule cell differentiation. *Dev. Biol.*, **322**, 345–354.

Kawauchi, D., Taniguchi, H., Watanabe, H., Saito, T. & Murakami, F. (2006) Direct visualization of nucleogenesis by precerebellar neurons: involvement of ventricle-directed, radial fibre-associated migration. *Development*, **133**, 1113–1123.

Kohda, K., Kakegawa, W., Matsuda, S., Nakagami, R., Kakiya, N. & Yuzaki, M. (2007) The extreme C-terminus of GluRdelta2 is essential for induction of long-term depression in cerebellar slices. *Eur. J. Neurosci.*, **25**, 1357–1362.

Kolk, S.M., de Mooij-Malsen, A.J. & Martens, G.J. (2011) Spatiotemporal molecular approach of *in utero* electroporation to functionally decipher endophenotypes in neurodevelopmental disorders. *Front. Mol. Neurosci.*, **4**, 37.

Lau, P., Bailey, P., Dowhan, D.H. & Muscat, G.E. (1999) Exogenous expression of a dominant negative RORalpha1 vector in muscle cells impairs differentiation: RORalpha1 directly interacts with p300 and myoD. *Nucleic Acids Res.*, **27**, 411–420.

Lau, P., Nixon, S.J., Parton, R.G. & Muscat, G.E. (2004) RORalpha regulates the expression of genes involved in lipid homeostasis in skeletal muscle cells: caveolin-3 and CPT-1 are direct targets of ROR. *J. Biol. Chem.*, **279**, 36828–36840.

Matsuda, T. & Cepko, C.L. (2004) Electroporation and RNA interference in the rodent retina *in vivo* and *in vitro*. *Proc. Natl. Acad. Sci. USA*, **101**, 16–22.

Matsuda, T. & Cepko, C.L. (2007) Controlled expression of transgenes introduced by *in vivo* electroporation. *Proc. Natl. Acad. Sci. USA*, **104**, 1027–1032.

Miale, I.L. & Sidman, R.L. (1961) An autoradiographic analysis of histogenesis in the mouse cerebellum. *Exp. Neurol.*, **4**, 277–296.

Miyazaki, T., Fukaya, M., Shimizu, H. & Watanabe, M. (2003) Subtype switching of vesicular glutamate transporters at parallel fibre-Purkinje cell synapses in developing mouse cerebellum. *Eur. J. Neurosci.*, **17**, 2563–2572.

Nakagawa, S., Watanabe, M., Isobe, T., Kondo, H. & Inoue, Y. (1998) Cytological compartmentalization in the staggerer cerebellum, as revealed by calbindin immunohistochemistry for Purkinje cells. *J. Comp. Neurol.*, **395**, 112–120.

Navarro-Quiroga, I., Chittajallu, R., Gallo, V. & Haydar, T.F. (2007) Long-term, selective gene expression in developing and adult hippocampal pyramidal neurons using focal *in utero* electroporation. *J. Neurosci.*, **27**, 5007–5011.

Oberdick, J., Smeyne, R.J., Mann, J.R., Zackson, S. & Morgan, J.I. (1990) A promoter that drives transgene expression in cerebellar Purkinje and retinal bipolar neurons. *Science*, **248**, 223–226.

Pierce, E.T. (1967) Histogenesis of the dorsal and ventral cochlear nuclei in the mouse. An autoradiographic study. *J. Comp. Neurol.*, **131**, 27–54.

Saito, T. & Nakatsuji, N. (2001) Efficient gene transfer into the embryonic mouse brain using *in vivo* electroporation. *Dev. Biol.*, **240**, 237–246.

Sidman, R.L., Lane, P.W. & Dickie, M.M. (1962) Staggerer, a new mutation in the mouse affecting the cerebellum. *Science*, **137**, 610–612.

Slemmer, J.E., De Zeeuw, C.I. & Weber, J.T. (2005) Don't get too excited: mechanisms of glutamate-mediated Purkinje cell death. *Prog. Brain Res.*, **148**, 367–390.

Smeyne, R.J., Oberdick, J., Schilling, K., Berrebi, A.S., Mugnaini, E. & Morgan, J.I. (1991) Dynamic organization of developing Purkinje cells revealed by transgene expression. *Science*, **254**, 719–721.

Soha, J.M. & Herrup, K. (1995) Stunted morphologies of cerebellar Purkinje cells in lurcher and staggerer mice are cell-intrinsic effects of the mutant genes. *J. Comp. Neurol.*, **357**, 65–75.

Sotelo, C. & Dusart, I. (2009) Intrinsic versus extrinsic determinants during the development of Purkinje cell dendrites. *Neuroscience*, **162**, 589–600.

Tabata, H. & Nakajima, K. (2001) Efficient *in utero* gene transfer system to the developing mouse brain using electroporation: visualization of neuronal migration in the developing cortex. *Neuroscience*, **103**, 865–872.

Takayama, K., Torashima, T., Horiuchi, H. & Hirai, H. (2008) Purkinje-cell-preferential transduction by lentiviral vectors with the murine stem cell virus promoter. *Neurosci. Lett.*, **443**, 7–11.

Tamada, A., Kumada, T., Zhu, Y., Matsumoto, T., Hatanaka, Y., Muguruma, K., Chen, Z., Tanabe, Y., Torigoe, M., Yamauchi, K., Oyama, H., Nishida, K. & Murakami, F. (2008) Crucial roles of Robo proteins in midline crossing of cerebellofugal axons and lack of their up-regulation after midline crossing. *Neural Dev.*, **3**, 29.

Terashima, T., Miwa, A., Kanegae, Y., Saito, I. & Okado, H. (1997) Retrograde and anterograde labeling of cerebellar afferent projection by the injection of recombinant adenoviral vectors into the mouse cerebellar cortex. *Anat. Embryol. (Berl)*, **196**, 363–382.

Tomomura, M., Rice, D.S., Morgan, J.I. & Yuzaki, M. (2001) Purification of Purkinje cells by fluorescence-activated cell sorting from transgenic mice that express green fluorescent protein. *Eur. J. Neurosci.*, **14**, 57–63.

Torashima, T., Okoyama, S., Nishizaki, T. & Hirai, H. (2006) *In vivo* transduction of murine cerebellar Purkinje cells by HIV-derived lentiviral vectors. *Brain Res.*, **1082**, 11–22.

Wang, V.Y. & Zoghbi, H.Y. (2001) Genetic regulation of cerebellar development. *Nat. Rev. Neurosci.*, **2**, 484–491.

Wang, V.Y., Rose, M.F. & Zoghbi, H.Y. (2005) Math1 expression redefines the rhombic lip derivatives and reveals novel lineages within the brainstem and cerebellum. *Neuron*, **48**, 31–43.

Wu, Z., Yang, H. & Colosi, P. (2010) Effect of genome size on AAV vector packaging. *Mol. Ther.*, **18**, 80–86.

Yuzaki, M. (2005) Transgenic rescue for characterizing orphan receptors: a review of delta2 glutamate receptor. *Transgenic Res.*, **14**, 117–121.

Zimmermann, T., Rietdorf, J. & Pepperkok, R. (2003) Spectral imaging and its applications in live cell microscopy. *FEBS Lett.*, **546**, 87–92.